

# One-Pot Covalent Functionalization of 2D Black Phosphorus by Anionic Ring Opening Polymerization

Obida Bawadkji, Mariam Cherri, Andreas Schäfer, Svenja Herziger, Philip Nickl, Katharina Achazi, Ievgen S. Donskyi,\* Mohsen Adeli,\* and Rainer Haag\*

**In this work, a one-pot approach for the covalent functionalization of few-layer black phosphorus (BP) by anionic ring opening polymerization of glycidol to obtain multifunctional BP-polyglycerol (BP-PG) with high amphiphilicity for near-infrared-responsive drug delivery and biocompatibility is reported. Straightforward synthesis in combination with exceptional biological and physicochemical properties designates functionalized BP-PG as a promising candidate for a broad range of biomedical applications.**

## 1. Introduction

Since the first successful isolation of few-layer black phosphorus (BP) in 2014, it has attracted a great deal of attention for a broad range of applications.<sup>[1–6]</sup> BP is a member of the 2D nanomaterial family, distinguished with anisotropic features and low-toxic biodegradation.<sup>[7,8]</sup> Owing to its layer-dependent and tunable bandgap,<sup>[9,10]</sup> direction-dependent Young's modulus,<sup>[11]</sup> and excellent carrier mobility<sup>[12]</sup> as well as ON–OFF ratio,<sup>[13,14]</sup> BP is a promising pnictogen candidate for

a wide range of biomedical applications, including drug delivery, photodynamic therapy, photothermal therapy (PTT), bioimaging, biosensing, theranostics, and bone-/neuro-regeneration.<sup>[4,15–27]</sup> One of the inherent features of BP is its degradation to low-toxic phosphorus species such as phosphates, phosphites, and other  $P_xO_y$  compounds by reacting with oxygen.<sup>[8,28–30]</sup> whereas other 2D nanomaterials do not degrade in biological mediums and cause health problems upon in vivo applica-


tions.<sup>[31,32]</sup> Biomedical applications of BP, however, are restricted by its low-dispersibility, agglomeration, and rapid degradation in aqueous mediums.<sup>[29,33–35]</sup> The surface of BP is hydrophobic and becomes only slightly hydrophilic upon degradation by forming  $P_xO_y$  species.<sup>[28]</sup> Consequently, the biomedically useful form of non-degraded BP is not able to be successfully distributed within biological media. Successful implementation of BP for biomedical applications necessitates a homogeneous distribution of the BP nanomaterials in aqueous systems without the formation of aggregations which can lead to various complications, preventing cellular uptake due to the nanoparticle size increase.<sup>[36,37]</sup>

Modification of nanomaterials with polymers is performed mainly to enhance the biomedical applicability of the nanoparticle.<sup>[2,38,39]</sup> Polymer decoration can prevent nanoparticle agglomeration by increasing the steric hindrance, diminishing the surface energy, and neutralizing the surface charges of the host nanoparticles.<sup>[40,41]</sup> In the case of oxidative degradable systems, encapsulation of the nanoparticles with polymers can decrease the contact of the host nanoparticle to surrounding oxygen and water.<sup>[42,43]</sup> Additionally, hydrophilic polymers greatly increase the biodistribution of the nanoparticles and thus drastically enhance their biocompatibility.<sup>[44–46]</sup> Depending on the polymer modification, additional functions can be provided to the host systems, such as selective targeting abilities and gene delivery.<sup>[47,48]</sup> So far, various efforts have been devoted to obtain water-dispersible BP nanomaterials, however, most reported materials are polymeric composites based on non-covalent interactions rather than covalent bonding.<sup>[38,45,48–52]</sup> The main issue with such nanocomposites which rely on non-covalent interactions (i.e., electrostatic adsorption of polymers) is the desorption of the polymeric coating when implemented in biological media. The stability of polymeric coatings directly correlates to the biodistribution of the respective material.<sup>[40]</sup> Compared to non-covalent interactions, covalent functionalization of nanomaterials is

O. Bawadkji, M. Cherri, A. Schäfer, P. Nickl, K. Achazi, I. S. Donskyi, R. Haag  
Institut für Chemie und Biochemie  
Freie Universität Berlin  
Takustr. 3, 14195 Berlin, Germany  
E-mail: ievgen.donskyi@fu-berlin.de; haag@chemie.fu-berlin.de

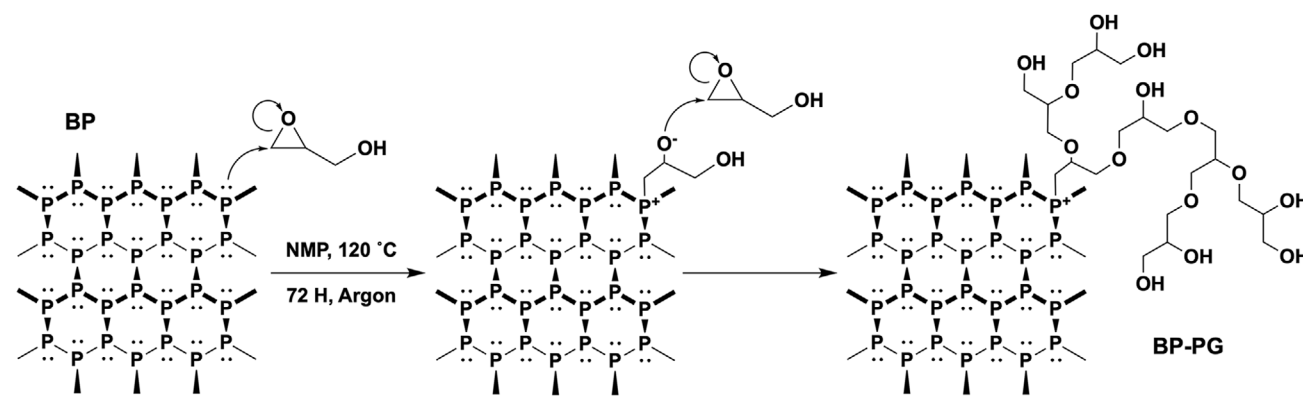
S. Herziger  
Forschungszentrum für Elektronenmikroskopie and Core Facility BioSupraMol  
Institut für Chemie und Biochemie  
Freie Universität Berlin  
Fabeckstr. 36a, 14195 Berlin, Germany  
P. Nickl, I. S. Donskyi  
BAM – Federal Institute for Material Science and Testing  
Division of Surface Analysis and Interfacial Chemistry  
Unter den Eichen 44–46, 12205 Berlin, Germany

M. Adeli  
Department of Chemistry  
Faculty of Science  
Lorestan University  
Khorramabad 6815144316, Iran  
E-mail: adeli.m@lu.ac.ir

 The ORCID identification number(s) for the author(s) of this article can be found under <https://doi.org/10.1002/admi.202201245>.

© 2022 The Authors. Advanced Materials Interfaces published by Wiley-VCH GmbH. This is an open access article under the terms of the Creative Commons Attribution License, which permits use, distribution and reproduction in any medium, provided the original work is properly cited.

DOI: 10.1002/admi.202201245



**Scheme 1.** Anionic ring-opening polymerization of glycidol by BP, forming BP-PG.

considered to be more stable.<sup>[38]</sup> Recent studies have shown that BP can be covalently functionalized by reactive chemical species.<sup>[53–63]</sup> For example, aryl derivatives have been successfully attached to the surface of BP nanosheets using aryl diazonium precursors. Covalent attachment of these chemical species to the surface of BP nanoflakes has drastically altered their stability and electronic properties.<sup>[53,64]</sup> Alkyl chains have also been conjugated to the surface of BP nanoflakes by a nucleophilic substitution reaction between BP and alkyl iodides.<sup>[62]</sup> Amination of BP nanosheets via nucleophilic substitution followed by a reaction with epoxy resin resulted in novel nanocomposites through a multistep pathway.<sup>[65]</sup> The above-mentioned reactions, however, rely on a “grafting-to” approach through which the (macro)molecule is converted to a reactive reagent and then associated to create 2D platforms via different pathways. Functionalization of 2D nanomaterials using the “grafting-from” approach is a straightforward method to produce new materials,<sup>[66]</sup> in which polymerization of monomers is initiated from the surface of the 2D nanoplatform and continued by self-propagation.<sup>[67]</sup> This approach improves functionality, water-dispersibility, and physiochemical properties of 2D platforms for different biomedical applications.<sup>[68]</sup> A possible way to allow the use of BP in biological applications is to functionalize BP nanomaterials covalently with hydrophilic (macro)molecules.<sup>[2,38]</sup> Hyperbranched polyglycerol (hPG) is a polyfunctional macromolecule that holds many advantages over its analogues and has been used in a wide range of biomedical applications since its first synthesis in 1966 by Sandler and Berg.<sup>[69–74]</sup> High functionality, high water solubility, and resistance to protein adsorption paired with long blood circulation time designate hPG as a unique candidate for in vivo applications.<sup>[72,75]</sup> Covalent functionalization of BP nanomaterials improves their dispersibility in aqueous solutions and inhibits their aggregation,<sup>[2,38]</sup> and can also decrease the toxicity of BP nanomaterials by reducing their polydispersity in terms of lateral dimensions and thickness.<sup>[76]</sup> So far, efforts to achieve covalently functionalized polymer-based BP nanomaterials are limited to few examples.<sup>[38,77–79]</sup>

In this work, we report on a one-pot “grafting-from” approach for the covalent functionalization of BP with hPG. Taking advantage of the nucleophilicity of phosphorus atoms, anionic ring-opening polymerization of glycidol was initiated from the surface of BP nanoflakes and a 2D platform

consisting of a BP backbone and polyglycerol coating was obtained. The polyglycerol-functionalized BP nanoflakes (BP-PG) showed high water dispersibility, biocompatibility, and efficient cellular uptake.

## 2. Results and Discussion

BP nanoflakes were prepared via liquid-phase exfoliation in *N*-methyl-2-pyrrolidone (NMP) (ESI)<sup>[80]</sup> and used for subsequent functionalization with polyglycerol via a one-pot anionic ring-opening polymerization of glycidol (ESI). Polymerization of glycidol was initiated by nucleophilic attack of phosphorus atoms and propagated by alkoxy-mediated polymerization. BP nanoflakes were incubated with glycidol at 120 °C for 72 h (**Scheme 1**) and the product of the reaction after purification was characterized by different spectroscopic and microscopic methods as well as thermal analysis.

Solid-state <sup>31</sup>P magic-angle spinning nuclear magnetic resonance (<sup>31</sup>P-MAS-NMR) spectrum (**Figure 1a**) showed a sharp signal, accompanied by spinning sidebands (SSBs), at 19.0 ppm corresponding to non-functionalized BP.<sup>[81]</sup> With higher rotational speed, the SSBs shifted further apart, and with total suppression of SSBs (TOSS), they disappeared (**Figure S1**, Supporting Information). Both results proved that the corresponding signals did not originate from impurities or degraded BP. BP-PG, on the other hand, showed a new signal at ≈23.8 ppm, which corresponded to the newly formed P–C covalent bond (**Figure 1b**).<sup>[62]</sup> This bond was formed by a nucleophilic reaction between phosphorus atoms of BP and carbon atoms of the epoxide ring of glycidol. This result supports the covalent functionalization of BP.<sup>[62]</sup> The percentage of functionalized BP atoms (BP-PG) to non-functionalized BP atoms (pure BP) was quantified to be ≈8.0% (**Figure S2**, Supporting Information). Assuming comparable relaxation times for both phosphorous species, and by line fitting of the <sup>31</sup>P-MAS-NMR spectrum, the integral ratio of the two peaks following Equation (1) was determined:

$$\text{BP-PG}\% = \left( \frac{\int \text{BP-PG}}{\int \text{BP} + \int \text{BP-PG}} \right) \times 100 \quad (1)$$

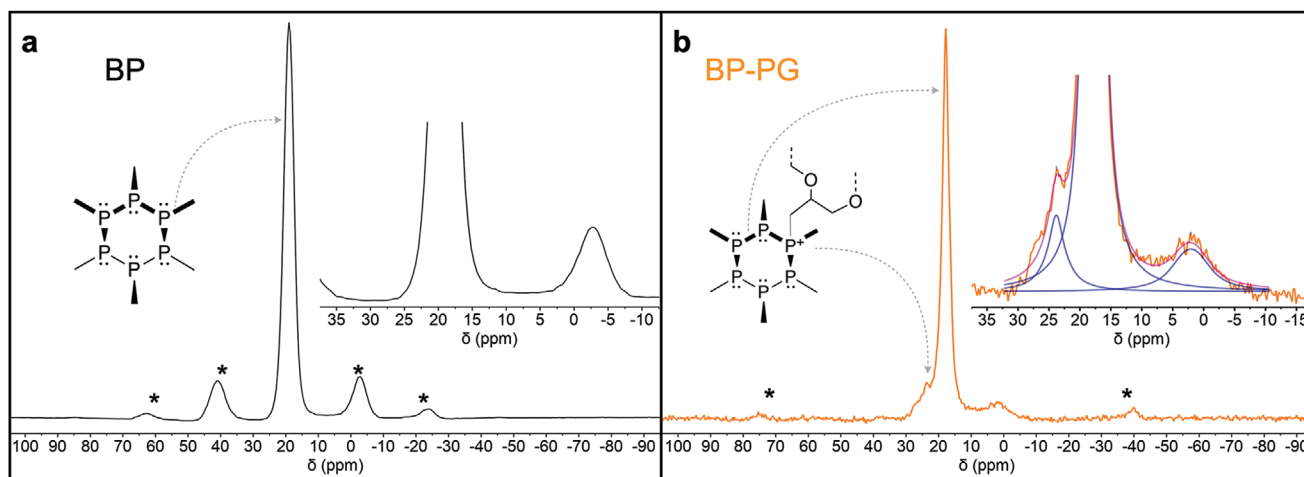


**Figure 1.**  $^{31}\text{P}$ -MAS-NMR spectra of a) BP and b) BP-PG with spectrum insets (\* indicate SSBs, blue lines indicate line fitting for BP-PG's spectrum).

On the other hand,  $^1\text{H}$  and  $^{13}\text{C}$  NMR spectroscopy in deuterium oxide ( $\text{D}_2\text{O}$ ) indicated signals for the polyglycerol component of BP-PG (Figure 2a and Figure S3, Supporting Information).<sup>[82]</sup> As a proof-of-concept, the possibility of the glycidol's epoxide ring to be opened by the lone-pair of electrons from a phosphorus atom was investigated by a model reaction using triphenylphosphine ( $\text{PPh}_3$ ) (Figure S11, Supporting Information).<sup>[83]</sup> Further characterization of BP and

BP-PG was conducted via Raman spectroscopy (Figure 2b). Raman spectrum of BP showed vibration modes at 363, 438, and 467  $\text{cm}^{-1}$  corresponding to the characteristic  $A_g^1$ ,  $B_{2g}$ , and  $A_g^2$  vibrational modes of few-layer BP, respectively.<sup>[7]</sup> Compared to the bare BP, vibrational modes of BP-PG were attenuated due to its polyglycerol coverage. X-ray photoelectron spectroscopy (XPS) was also used to investigate the chemical composition of the materials. Survey XPS analysis (Table S1, Supporting

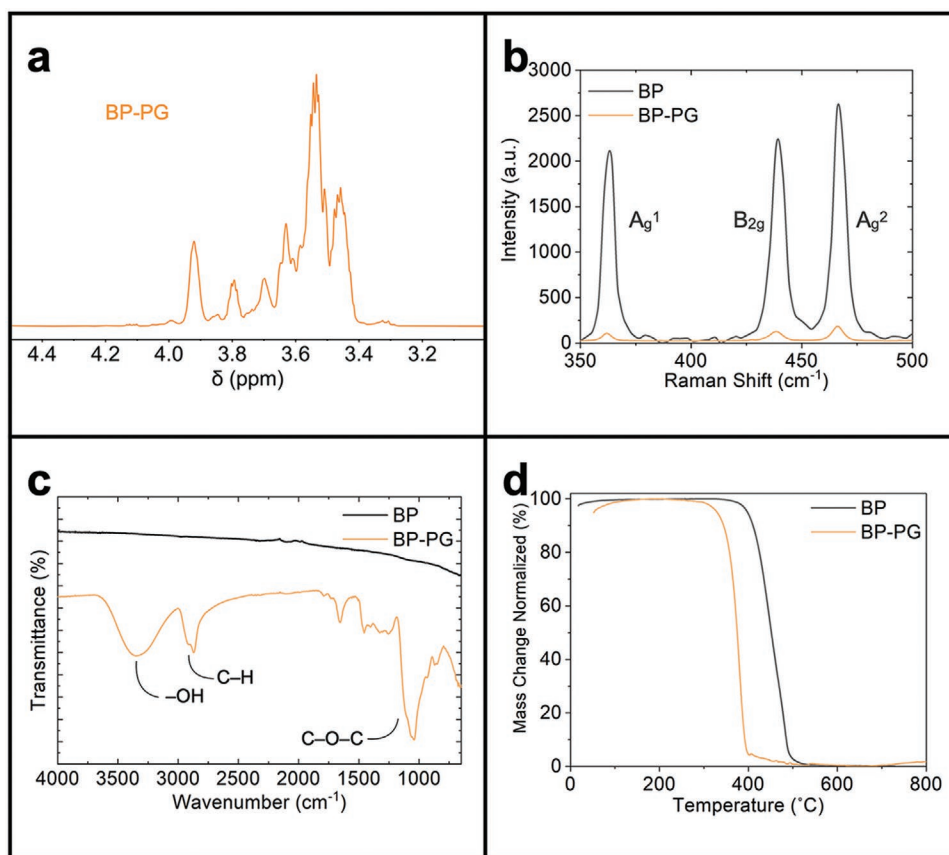


**Figure 2.** a)  $^1\text{H}$ -NMR spectrum of BP-PG in  $\text{D}_2\text{O}$ . b) Raman and c) FT-IR spectra of BP and BP-PG. d) TGA thermograms of BP and BP-PG in argon.

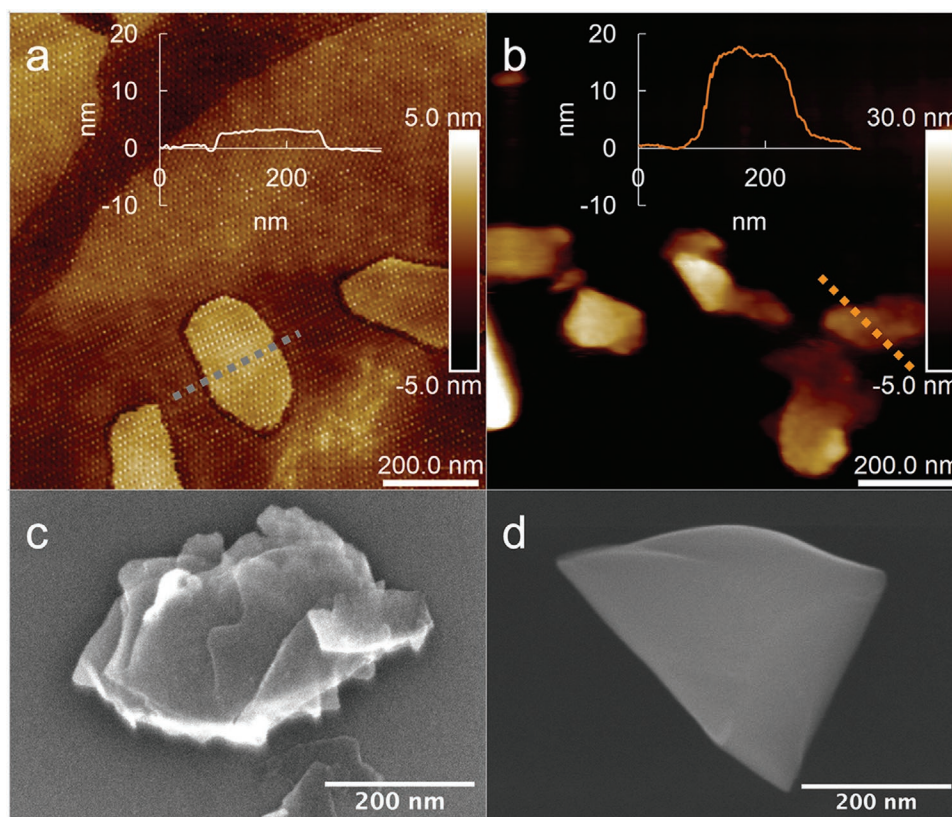


**Figure 3.** a,b) AFM and c,d) SEM images of BP and BP-PG, respectively. Both images showed sheet-like structures for functionalized and non-functionalized BP.

Information) of BP-PG revealed signals for carbon, and oxygen species. However, peaks for phosphorus were not detected because the thickness of the polymer coverage (Figure 3b) was greater than the detection depth limit of XPS devices (usually in the range of 5–10 nm).<sup>[84]</sup> In the Fourier transform infrared (FT-IR) spectrum of BP-PG (Figure 2c), absorbance bands at 3300, 2900, and 1100  $\text{cm}^{-1}$  were assigned to the hydroxyl groups (–OH), aliphatic C–H, and C–O–C stretching vibrations of the polyglycerol coverage, respectively.<sup>[85]</sup> These absorbance bands provided further support for the successful attachment of hPG to the surface of BP. Thermogravimetric analysis (TGA) under argon (Figure 2d) indicated a thermal decomposition starting from 400 °C for BP, whereas the main weight loss or decomposition of BP-PG occurred at 300 °C. Interestingly, thermograms of BP under air indicated a gain of mass starting from 250 °C (Figure S4, Supporting Information). This increase in mass corresponded to the reactions of phosphorus atoms with oxygen and formation of  $\text{P}_x\text{O}_y$  species.<sup>[86]</sup> The TGA thermogram of BP-PG under air revealed a two-step weight loss initiated at  $\approx 250$  °C for the decomposition of the hPG shell, followed by the thermal decomposition of the residues at  $\approx 350$  °C, similar to previously reported data.<sup>[64,86]</sup>

Atomic force microscopy (AFM) indicated that the BP sheets were in the few-layer regime (<10 nm thick) with an average lateral size of 200–300 nm. According to the AFM images, the average height of the nanoflakes was 3.8 nm, corresponding to  $\approx$  four layers of BP sheets (Figure 3a).<sup>[34]</sup> AFM images of BP-PG (Figure 3b) showed 2D platforms with an average thickness

of 15 nm. The lateral dimensions of BP-PG, in comparison with the non-functionalized BP sheets, did not significantly change. BP-PG nanoflakes, in many cases, were folded, which is a common observation for functionalized 2D nanomaterials (Figure S5a,b, Supporting Information).<sup>[66,87]</sup> Moreover, transmission electron microscopy (TEM) revealed aggregations for both BP and BP-PG with clear edges (Figure S5c,d, Supporting Information). TEM results were further elucidated by scanning electron microscopy (SEM). SEM images revealed few-layer nanoflakes with clear edges and lateral dimensions of a few hundred nanometers for BP. A smooth surface, assigned to the polymer shell, was observed for BP-PG (Figure 3c,d). These observations confirmed the successful polymerization of glycidol monomers on the surface of BP.

The dispersibility of BP-PG in aqueous physiological mediums was tested by UV–vis spectra of dispersions of both BP and BP-PG in phosphate-buffer saline solutions (pH 6.6 and 7.4) recorded over a period of 24 h. Decrease in the absorption of each dispersion was assigned to the sedimentation of the corresponding material (Figure S6, Supporting Information). After 24 h,  $\approx 80$ –90% of the BP-PG remained suspended in the aqueous media, whereas more than 96% of the non-functionalized BP dispersion precipitated. BP-PG was highly dispersible in aqueous solutions, as expected, due to the enhanced hydrophilicity provided by the polyglycerol coverage. Zeta potential analysis indicated a decrease in the surface charge of the non-functionalized BP (from  $-37.4$  to  $-78$  mV) upon functionalization with polyglycerol (Figure S7, Supporting Information).

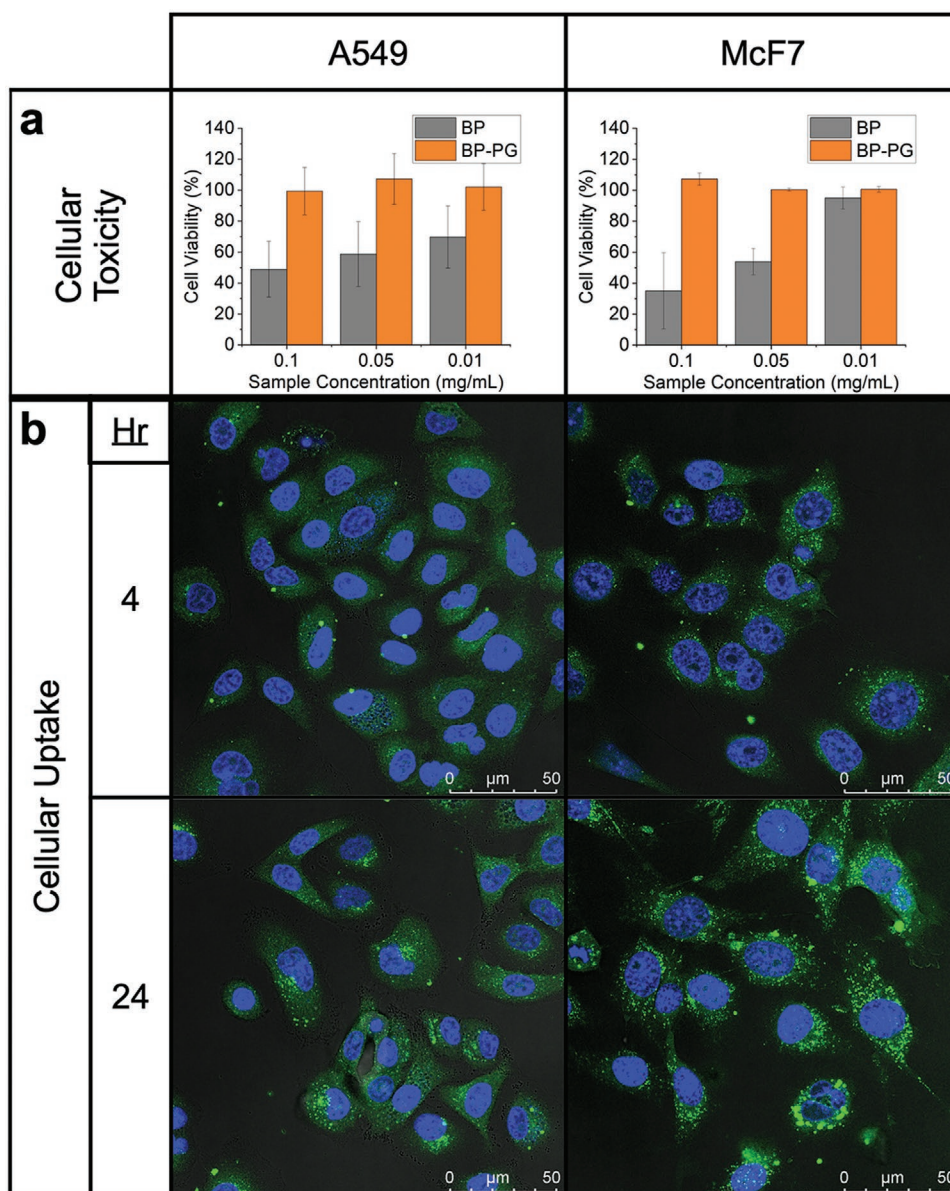


**Figure 4.** a) Cell viability of A549 and McF7 cells treated with BP and BP-PG at different concentrations assessed with the CCK8-Assay. Data represents mean  $\pm$  SD ( $n = 4$ ). b) Confocal microscopy images of A549 and McF7 cells incubated with dye-conjugated BP-PG-FITC ( $100 \mu\text{g mL}^{-1}$ ) after 4 and 24 h (Merged images; blue: Hoechst333342, green: FITC).

For the investigation of cell compatibility, A549, McF7 (Figure 4a), and HeLa (Figure S8, Supporting Information) cells were treated with BP-PG at different concentrations and their viability, to assess the potential of polyglycerol-functionalized BP for biomedical applications, was investigated. While BP-PG showed no significant impact on the cellular viability up to a concentration of  $0.1 \text{ mg mL}^{-1}$ , its non-functionalized counterpart showed a dose-dependent toxic effect with  $50 \pm 20\%$ ,  $80 \pm 40\%$ , and  $90 \pm 1\%$  loss of cell viability at  $0.1 \text{ mg mL}^{-1}$  for A549, McF7, and HeLa cell lines, respectively. At high concentrations of BP-PG ( $10 \text{ mg mL}^{-1}$ ), the cell viability was still  $75 \pm 8\%$ . These results demonstrated the significant impact of the polyglycerol shell on the biocompatibility of BP nanoflakes, nominating BP-PG as a biocompatible platform for biomedical applications.

To further investigate the biological behavior of BP-PG and study its cell penetration ability, its cellular uptake by the same cell lines was evaluated using confocal laser scanning microscopy (CLSM) (Figure 4b and Figure S9, Supporting Information). To track the uptake of BP-PG by cells, the platform was labeled with fluorescein 5-isothiocyanate (5-FITC). The optical properties of FITC labeled nanoflakes (BP-PG-FITC) were investigated by UV-vis and fluorescence spectroscopy (Figure S9c,d, Supporting Information). BP-PG-FITC was incubated with the above-mentioned cell lines for a total of 24 h and the signal of FITC was monitored by CLSM after 4 and 24 h. The green fluorescence emission inside the cells increased over time and accumulated close to the nucleus (blue), which indicated a time-dependent uptake for BP-PG-FITC. Moreover,

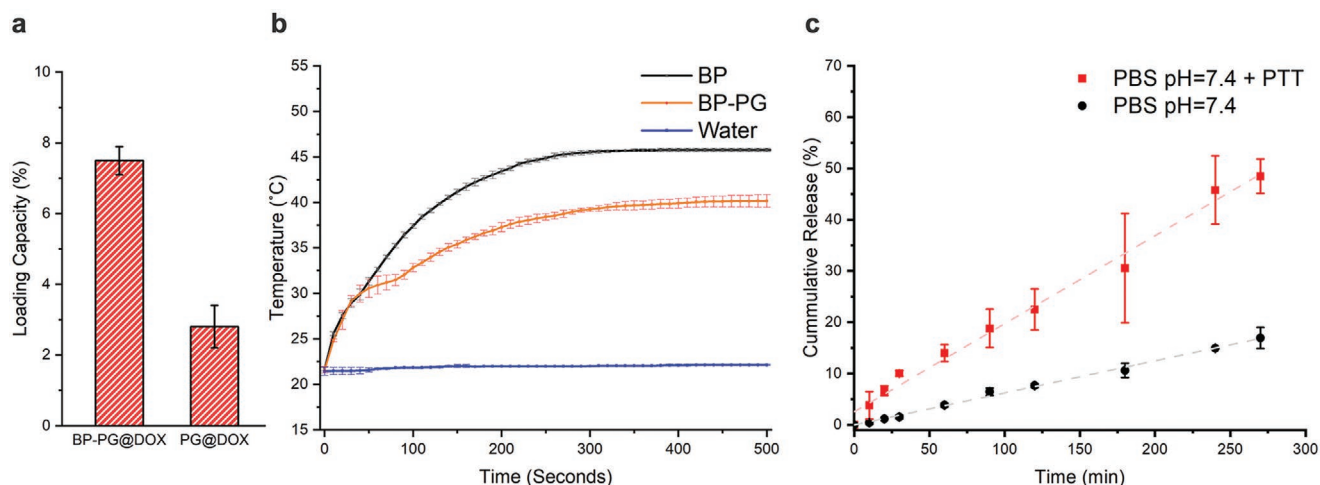


**Figure 5.** a) DOX loading capacity on BP-PG and pure PG. b) Photothermal testing of BP and BP-PG in water over 500 s using a fiber-optic laser (808 nm, 1 W cm<sup>-2</sup>). c) In vitro DOX release from BP-PG@DOX with and without NIR irradiation in PBS. All data represents mean ± SD (*n* = 3).

no morphological changes and other signs of adverse effects were observed after 24 h of incubation. These results indicate optimal cell compatibility for BP-PG owing to the increased hydrophilicity provided by the grafted polyglycerol.

Studies have shown that BP nanomaterials can be loaded with drug molecules for targeted therapy.<sup>[88,89]</sup> Owing to its puckered structure, BP nanomaterials provide a large surface area-to-volume ratio for highly efficient loading of therapeutic drugs.<sup>[90,91]</sup> Coupled with anisotropic properties and near-infrared irradiation (NIR) responsiveness, BP nanomaterials can be utilized as drug delivery platforms with on-demand release of the loaded therapeutic agent by local heating. Pure PG, on the other hand, is a highly hydrophilic molecule which poorly loads hydrophobic therapeutic agents, such as doxorubicin (DOX), in aqueous solution. To test whether BP-PG can be used as a drug delivery platform, an aqueous solution of BP-PG (10 mg mL<sup>-1</sup>) was added dropwise to a DOX solution and stirred overnight for a targeted loading capacity (LC) of 10%. In comparison, a control experiment was performed with pure PG instead of BP-PG to prove that DOX is loaded into BP-PG system through the interactions with BP. The LC was determined via UV-vis spectroscopy (Figure 5a) and has shown that for BP-PG@DOX LC = 7.5%, as for PG@DOX 2.8%. The presence of BP in the nanomaterials is essential to obtain a high loading efficiency of DOX.

One of the intrinsic properties of BP qualifying it for tumor therapy is its photothermal conversion capability. PTT is a new emerging anticancer therapy. The working mechanism relies in photothermal agents that can convert laser irradiation energy to heat under NIR irradiation which can degenerate tumor tissues.<sup>[92,93]</sup> Tao et al. has previously demonstrated that BP-based delivery platforms were able to enhance antitumor activities under PTT.<sup>[45]</sup> Accordingly, the photothermal property of BP-PG in aqueous dispersions was investigated (Figure 5b). After 6 min of laser irradiation (808 nm, 1 W cm<sup>-2</sup>), the temperature of the aqueous dispersion increased from 22 to 40 °C. For non-functionalized BP, the temperature of the aqueous media was similarly increased to 45 °C. Therefore, covalent functionalization with polyglycerol according to the described procedure does not drastically disrupt the photothermal conversion efficiency of BP nanomaterials.

Consequently, the BP-PG@DOX system was tested for its photothermal responsiveness under NIR irradiation and its ability to release the drug DOX in vitro. BP-PG@DOX (5 mg mL<sup>-1</sup>) contained in a dialysis kit was irradiated by an NIR laser. A sample was taken at different time periods and UV-vis spectroscopy was utilized to determine the cumulative release within 270 min (Figure 5c), and without NIR irradiation for 24 h (Figure S10, Supporting Information). In comparison, the same experimental setup was carried out without the exposure of BP-PG@DOX to NIR irradiation. Results show that after 270 min, BP-PG@DOX exposed to NIR irradiation was able to release around 50% of the encapsulated drug in comparison to 20% that has been leached out of the system with no exposure to NIR irradiation, highlighting the potentials for BP-PG to be used in on-demand targeted therapy.

### 3. Conclusion

In summary, few-layer BP is covalently functionalized with polyglycerol via a one-pot anionic ring-opening polymerization. The nucleophilicity of the phosphorus atoms of BP is strong enough to attack epoxide rings and initiate polymerization of a cyclic monomer such as glycidol. Due to its high water dispersibility, low toxicity, efficient cellular uptake, and photothermal conversion, polyglycerol-functionalized BP demonstrates a great potential for future biomedical applications.

### Supporting Information

Supporting Information is available from the Wiley Online Library or from the author.

### Acknowledgements

This study was supported by the Deutsche Forschungsgemeinschaft (DFG, German Research Foundation)—SFB 1449—projects A01, B03, C04, and Z02. Raman Spectroscopy was performed at the Department of Physics of Freie Universität Berlin contributed by Prof. Dr. Stephanie

Reich. The authors thank Prof. Dr. Christian Müller for the support that was provided and Elisa Quaas for performing cell viability and uptake experiments. The authors acknowledge Taylor Page for proofreading the manuscript, and Dr. Jörg Radnik and M. Eng. Jörg Stockmann from the BAM institute for support with the XPS measurements.

Open access funding enabled and organized by Projekt DEAL.

## Conflict of Interest

The authors declare no conflict of interest.

## Data Availability Statement

The data that support the findings of this study are available in the supplementary material of this article.

## Keywords

2D nanomaterials, amphiphilicity, black phosphorus, hyperbranched polyglycerol, water dispersibility

Received: June 3, 2022

Revised: August 10, 2022

Published online: September 16, 2022

- [1] G. Qu, T. Xia, W. Zhou, X. Zhang, H. Zhang, L. Hu, J. Shi, X.-F. Yu, G. Jiang, *Chem. Rev.* **2020**, *120*, 2288.
- [2] H. Liu, Y. Mei, Q. Zhao, A. Zhang, L. Tang, H. Gao, W. Wang, *Pharmaceutics* **2021**, *13*, 1344.
- [3] B. Li, C. Lai, G. Zeng, D. Huang, L. Qin, M. Zhang, M. Cheng, X. Liu, H. Yi, C. Zhou, F. Huang, S. Liu, Y. Fu, *Small* **2019**, *15*, 1804565.
- [4] J. R. Choi, K. W. Yong, J. Y. Choi, A. Nilghaz, Y. Lin, J. Xu, X. Lu, *Theranostics* **2018**, *8*, 1005.
- [5] M. Luo, T. Fan, Y. Zhou, H. Zhang, L. Mei, *Adv. Funct. Mater.* **2019**, *29*, 1808306.
- [6] Z. Hu, T. Niu, R. Guo, J. Zhang, M. Lai, J. He, L. Wang, W. Chen, *Nanoscale* **2018**, *10*, 21575.
- [7] A. Castellanos-Gomez, L. Vicarelli, E. Prada, J. O. Island, K. L. Narasimha-Acharya, S. I. Blanter, D. J. Groenendijk, M. Buscema, G. A. Steele, J. V. Alvarez, H. W. Zandbergen, J. J. Palacios, H. S. J. van der Zant, *2D Mater.* **2014**, *1*, 025001.
- [8] J. O. Island, G. A. Steele, H. S. J. van der Zant, A. Castellanos-Gomez, *2D Mater.* **2015**, *2*, 011002.
- [9] Z.-C. Luo, M. Liu, Z.-N. Guo, X.-F. Jiang, A.-P. Luo, C.-J. Zhao, X.-F. Yu, W.-C. Xu, H. Zhang, *Opt. Express* **2015**, *23*, 20030.
- [10] V. Tran, R. Soklaski, Y. Liang, L. Yang, *Phys. Rev. B* **2014**, *89*, 235319.
- [11] L. Kou, C. Chen, S. C. Smith, *J. Phys. Chem. Lett.* **2015**, *6*, 2794.
- [12] S. Cui, H. Pu, S. A. Wells, Z. Wen, S. Mao, J. Chang, M. C. Hersam, *J. Chem. Nat. Commun.* **2015**, *6*, 8632.
- [13] L. Li, Y. Yu, G. J. Ye, Q. Ge, X. Ou, H. Wu, D. Feng, X. H. Chen, Y. Zhang, *Nat. Nanotechnol.* **2014**, *9*, 372.
- [14] H. Liu, A. T. Neal, Z. Zhu, Z. Luo, X. Xu, D. Tománek, P. D. Ye, *ACS Nano* **2014**, *8*, 4033.
- [15] R. Gui, H. Jin, Z. Wang, J. Li, *Chem. Soc. Rev.* **2018**, *47*, 6795.
- [16] X. Ren, Z. Li, Z. Huang, D. Sang, H. Qiao, X. Qi, J. Li, J. Zhong, H. Zhang, *Adv. Funct. Mater.* **2017**, *27*, 1606834.
- [17] S. Anju, J. Ashtami, P. V. Mohanan, *Mater. Sci. Eng., C* **2019**, *97*, 978.
- [18] Y. T. Yew, Z. Sofer, C. C. Mayorga-Martinez, M. Pumera, *Mater. Chem. Front.* **2017**, *1*, 1130.
- [19] K. Huang, J. Wu, Z. Gu, *ACS Appl. Mater. Interfaces* **2019**, *11*, 2908.
- [20] M. Qiu, D. Wang, W. Liang, L. Liu, Y. Zhang, X. Chen, D. K. Sang, C. Xing, Z. Li, B. Dong, F. Xing, D. Fan, S. Bao, H. Zhang, Y. Cao, *Proc. Natl. Acad. Sci. USA* **2018**, *115*, 501.
- [21] M. Qiu, W. X. Ren, T. Jeong, M. Won, G. Y. Park, D. K. Sang, L.-P. Liu, H. Zhang, J. S. Kim, *Chem. Soc. Rev.* **2018**, *47*, 5588.
- [22] J. Ouyang, C. Feng, X. Zhang, N. Kong, W. Tao, *Acc. Mater. Res.* **2021**, *2*, 489.
- [23] J. Ouyang, X. Ji, X. Zhang, C. Feng, Z. Tang, N. Kong, A. Xie, J. Wang, X. Sui, L. Deng, Y. Liu, J. S. Kim, Y. Cao, W. Tao, *Proc. Natl. Acad. Sci. U. S. A.* **2020**, *117*, 28667.
- [24] C. Liu, J. Shin, S. Son, Y. Choe, N. Farokhzad, Z. Tang, Y. Xiao, N. Kong, T. Xie, J. S. Kim, W. Tao, *Chem. Soc. Rev.* **2021**, *50*, 2260.
- [25] Z. Tang, N. Kong, J. Ouyang, C. Feng, N. Y. Kim, X. Ji, C. Wang, O. C. Farokhzad, H. Zhang, W. Tao, *Matter* **2020**, *2*, 297.
- [26] M. Qiu, Y. Duo, W. Liang, Y. Yang, B. Zhang, Z. Xie, X. Yang, G. Wang, N. Xie, G. Nie, O. A. Alhartomy, A. A. ALGhamdi, S. Wageh, Y. Cao, H. Zhang, *Adv. Funct. Mater.* **2021**, *31*, 2104607.
- [27] M. Qiu, D. Wang, H. Huang, T. Yin, W. Bao, B. Zhang, Z. Xie, N. Xie, Z. Wu, C. Ge, Q. Wang, M. Gu, H. L. Kutscher, L. Liu, S. Bao, P. N. Prasad, H. Zhang, *Adv. Mater.* **2021**, *33*, 2102562.
- [28] Y. Huang, J. Qiao, K. He, S. Bliznakov, E. Sutter, X. Chen, D. Luo, F. Meng, D. Su, J. Decker, W. Ji, R. S. Ruoff, P. Sutter, *Chem. Mater.* **2016**, *28*, 8330.
- [29] J. Shao, H. Xie, H. Huang, Z. Li, Z. Sun, Y. Xu, Q. Xiao, X.-F. Yu, Y. Zhao, H. Zhang, H. Wang, P. K. Chu, *Nat. Commun.* **2016**, *7*, 12967.
- [30] T. Zhang, Y. Wan, H. Xie, Y. Mu, P. Du, D. Wang, X. Wu, H. Ji, L. Wan, *J. Am. Chem. Soc.* **2018**, *140*, 7561.
- [31] T. Liu, Y. Chao, M. Gao, C. Liang, Q. Chen, G. Song, L. Cheng, Z. Liu, *Nano Res.* **2016**, *9*, 3003.
- [32] S. S. An, S.-Y. Wu, J. Hulme, *Int. J. Nanomed.* **2015**, *10*, 9.
- [33] A. Ziletti, A. Carvalho, D. K. Campbell, D. F. Coker, A. H. Castro Neto, *Phys. Rev. Lett.* **2015**, *114*, 046801.
- [34] Z. Guo, H. Zhang, S. Lu, Z. Wang, S. Tang, J. Shao, Z. Sun, H. Xie, H. Wang, X.-F. Yu, P. K. Chu, *Adv. Funct. Mater.* **2015**, *25*, 6996.
- [35] X. Ding, Z. Wei, Y. Chen, P. Lin, Q. Yan, Y. Fan, X. Chen, Z. Cheng, *Opt. Mater. Express* **2019**, *9*, 423.
- [36] T. Welzel, I. Radtke, W. Meyer-Zaika, R. Heumann, M. Eppler, *J. Mater. Chem.* **2004**, *14*, 2213.
- [37] J. E. Skebo, C. M. Grabinski, A. M. Schrand, J. J. Schlager, S. M. Hussain, *Int. J. Toxicol.* **2007**, *26*, 135.
- [38] G. Zeng, Y. Chen, *Acta Biomater.* **2020**, *118*, 1.
- [39] A. N. Lukyanov, V. P. Torchilin, *Adv. Drug Delivery Rev.* **2004**, *56*, 1273.
- [40] D. H. Napper, *Polymeric Stabilization of Colloidal Dispersions*, Academic Press, London **1983**.
- [41] A. S. Dunn, *Br. Polym. J.* **1986**, *18*, 278.
- [42] F. Wu, M. Zhang, X. Chu, Q. Zhang, Y. Su, B. Sun, T. Lu, N. Zhou, J. Zhang, J. Wang, X. Yi, *Chem. Eng. J.* **2019**, *370*, 387.
- [43] W. Pan, C. Dai, Y. Li, Y. Yin, L. Gong, J. O. Machuki, Y. Yang, S. Qiu, K. Guo, F. Gao, *Biomaterials* **2020**, *239*, 119851.
- [44] C. Sun, Y. Xu, L. Deng, H. Zhang, Q. Sun, C. Zhao, Z. Li, *ACS Appl. Bio Mater.* **2018**, *1*, 673.
- [45] W. Tao, X. Zhu, X. Yu, X. Zeng, Q. Xiao, X. Zhang, X. Ji, X. Wang, J. Shi, H. Zhang, L. Mei, *Adv. Mater.* **2017**, *29*, 1603276.
- [46] D. Braatz, M. Cherri, M. Tully, M. Dimde, G. Ma, E. Mohammadifar, F. Reisbeck, V. Ahmadi, M. Schirner, R. Haag, *Angew. Chem. Int. Ed.* **2022**, e202203942.
- [47] X. Yang, D. Wang, Y. Shi, J. Zou, Q. Zhao, Q. Zhang, W. Huang, J. Shao, X. Xie, X. Dong, *ACS Appl. Mater. Interfaces* **2018**, *10*, 12431.
- [48] H. Wang, L. Zhong, Y. Liu, X. Xu, C. Xing, M. Wang, S.-M. Bai, C.-H. Lu, H.-H. Yang, *Chem. Commun.* **2018**, *54*, 3142.
- [49] W. Ou, J. H. Byeon, R. K. Thapa, S. K. Ku, C. S. Yong, J. O. Kim, *ACS Nano* **2018**, *12*, 10061.

- [50] H. Zhao, H. Chen, Z. Guo, W. Zhang, H. Yu, Z. Zhuang, H. Zhong, Z. Liu, *Chem. Eng. J.* **2020**, *394*, 124314.
- [51] N. Gao, J. Nie, H. Wang, C. Xing, L. Mei, W. Xiong, X. Zeng, Z. Peng, *J. Biomed. Nanotechnol.* **2018**, *14*, 1883.
- [52] X. Yang, D. Wang, J. Zhu, L. Xue, C. Ou, W. Wang, M. Lu, X. Song, X. Dong, *Chem. Sci.* **2019**, *10*, 3779.
- [53] C. R. Ryder, J. D. Wood, S. A. Wells, Y. Yang, D. Jariwala, T. J. Marks, G. C. Schatz, M. C. Hersam, *Nat. Chem.* **2016**, *8*, 597.
- [54] Y. Zhao, L. Tong, Z. Li, N. Yang, H. Fu, L. Wu, H. Cui, W. Zhou, J. Wang, H. Wang, P. K. Chu, X.-F. Yu, *Chem. Mater.* **2017**, *29*, 7131.
- [55] Y. Cao, X. Tian, J. Gu, B. Liu, B. Zhang, S. Song, F. Fan, Y. Chen, *Angew. Chem., Int. Ed.* **2018**, *57*, 4543.
- [56] L. Zhang, L.-F. Gao, L. Li, C.-X. Hu, Q.-Q. Yang, Z.-Y. Zhu, R. Peng, Q. Wang, Y. Peng, J. Jin, H.-L. Zhang, *Mater. Chem. Front.* **2018**, *2*, 1700.
- [57] W. Chen, S. Gao, Z. Xie, Y. Lu, G. Gong, G. Liu, J. Shang, C. Yao, R.-W. Li, *J. Mater. Chem. C* **2020**, *8*, 7309.
- [58] M. van Druenen, F. Davitt, T. Collins, C. Glynn, C. O'Dwyer, J. D. Holmes, G. Collins, *Chem. Mater.* **2018**, *30*, 4667.
- [59] X. Tang, W. Liang, J. Zhao, Z. Li, M. Qiu, T. Fan, C. S. Luo, Y. Zhou, Y. Li, Z. Guo, D. Fan, H. Zhang, *Small* **2017**, *13*, 1702739.
- [60] Q. Li, Q. Zhou, X. Niu, Y. Zhao, Q. Chen, J. Wang, *J. Phys. Chem. Lett.* **2016**, *7*, 4540.
- [61] Z. Sofer, J. Luxa, D. Bouša, D. Sedmidubský, P. Lazar, T. Hartman, H. Hardtdegen, M. Pumera, *Angew. Chem., Int. Ed.* **2017**, *56*, 9891.
- [62] S. Wild, M. Fickert, A. Mitrovic, V. Lloret, C. Neiss, J. A. Vidal-Moya, M. Á. Rivero-Crespo, A. Leyva-Pérez, K. Werbach, H. Peterlik, M. Grabau, H. Wittkämper, C. Papp, H.-P. Steinrück, T. Pichler, A. Görling, F. Hauke, G. Abellán, A. Hirsch, *Angew. Chem., Int. Ed.* **2019**, *58*, 5763.
- [63] H. Hu, H. Gao, L. Gao, F. Li, N. Xu, X. Long, Y. Hu, J. Jin, J. Ma, *Nanoscale* **2018**, *10*, 5834.
- [64] A. E. Del Río Castillo, C. D. Reyes-Vazquez, L. E. Rojas-Martinez, S. B. Thorat, M. Serri, A. L. Martinez-Hernandez, C. Velasco-Santos, V. Pellegrini, F. Bonaccorso, *FlatChem* **2019**, *18*, 100131.
- [65] S. Lin, B. Tao, X. Zhao, G. Chen, D.-Y. Wang, *Polymers* **2021**, *13*, 3635.
- [66] A. Faghani, M. F. Gholami, M. Trunk, J. Müller, P. Pachfule, S. Vogl, I. Donskyi, M. Li, P. Nickl, J. Shao, M. R. S. Huang, W. E. S. Unger, R. Arenal, C. T. Koch, B. Paulus, J. P. Rabe, A. Thomas, R. Haag, M. Adeli, *J. Am. Chem. Soc.* **2020**, *142*, 12976.
- [67] Z. Soury, M. Adeli, E. Mehdipour, A. Yari, A. Shams, S. Beyranvand, S. Sattari, *Langmuir* **2021**, *37*, 3382.
- [68] I. S. Donskyi, W. Azab, J. L. Cuellar-Camacho, G. Guday, A. Lippitz, W. E. S. Unger, K. Osterrieder, M. Adeli, R. Haag, *Nanoscale* **2019**, *11*, 15804.
- [69] A. Sunder, R. Hanselmann, H. Frey, R. Mülhaupt, *Macromolecules* **1999**, *32*, 4240.
- [70] D. Wilms, S.-E. Stiriba, H. Frey, *Acc. Chem. Res.* **2010**, *43*, 129.
- [71] R. K. Kainthan, S. R. Hester, E. Levin, D. V. Devine, D. E. Brooks, *Biomaterials* **2007**, *28*, 4581.
- [72] R. K. Kainthan, D. E. Brooks, *Biomaterials* **2007**, *28*, 4779.
- [73] H. Türk, A. Shukla, P. C. A. Rodrigues, H. Rehage, R. Haag, *Chem. - Eur. J.* **2007**, *13*, 4187.
- [74] R. K. Kainthan, Y. Zou, M. Chiao, J. N. Kizhakkedathu, *Langmuir* **2008**, *24*, 4907.
- [75] S. Abbina, S. Vappala, P. Kumar, E. M. J. Siren, C. C. La, U. Abbasi, D. E. Brooks, J. N. Kizhakkedathu, *J. Mater. Chem. B* **2017**, *5*, 9249.
- [76] M. Biedulska, P. Jakóbczyk, M. Sosnowska, B. Dec, A. Muchlińska, A. J. Zaczek, D. Nidzworski, R. Bogdanowicz, *Sci. Rep.* **2021**, *11*, 9304.
- [77] C. Sun, L. Wen, J. Zeng, Y. Wang, Q. Sun, L. Deng, C. Zhao, Z. Li, *Biomaterials* **2016**, *91*, 81.
- [78] L. Deng, Y. Xu, C. Sun, B. Yun, Q. Sun, C. Zhao, Z. Li, *Sci. Bull.* **2018**, *63*, 917.
- [79] D. An, J. Fu, Z. Xie, C. Xing, B. Zhang, B. Wang, M. Qiu, *J. Mater. Chem. B* **2020**, *8*, 7076.
- [80] J. R. Brent, N. Savjani, E. A. Lewis, S. J. Haigh, D. J. Lewis, P. O'Brien, *Chem. Commun.* **2014**, *50*, 13338.
- [81] S. Lange, P. Schmidt, T. Nilges, *Inorg. Chem.* **2007**, *46*, 4028.
- [82] M. Adeli, N. Mirab, M. S. Alavidjeh, Z. Sobhani, F. Atyabi, *Polymer* **2009**, *50*, 3528.
- [83] F. Plénat, D. Grelet, V. Ozon, H.-J. Cristau, *Synlett* **1994**, *1994*, 269.
- [84] C. Perruchot, J. F. Watts, C. Lowe, R. G. White, P. J. Cumpson, *Surf. Interface Anal.* **2002**, *33*, 869.
- [85] Z. Shen, S. Sun, W. Wang, J. Liu, Z. Liu, J. C. Yu, *J. Mater. Chem. A* **2015**, *3*, 3285.
- [86] J. Gómez-Pérez, B. Barna, I. Y. Tóth, Z. Kónya, Á. Kukovecz, *ACS Omega* **2018**, *3*, 12482.
- [87] S.-Y. Son, J.-M. Yun, Y.-J. Noh, S. Lee, H.-N. Jo, S.-I. Na, H.-I. Joh, *Carbon* **2015**, *81*, 546.
- [88] W. Chen, J. Ouyang, H. Liu, M. Chen, K. Zeng, J. Sheng, Z. Liu, Y. Han, L. Wang, J. Li, L. Deng, Y.-N. Liu, S. Guo, *Adv. Mater.* **2017**, *29*, 1603864.
- [89] W. Zhou, H. Cui, L. Ying, X.-F. Yu, *Angew. Chem., Int. Ed.* **2018**, *57*, 10268.
- [90] Z. Xie, D. Wang, T. Fan, C. Xing, Z. Li, W. Tao, L. Liu, S. Bao, D. Fan, H. Zhang, *J. Mater. Chem. B* **2018**, *6*, 4747.
- [91] Y. Huang, R. Li, Y. Dai, C. Qin, J. He, S. Yang, T. Wang, Y. Su, L. Jia, W. Zhao, *Mater. Des.* **2022**, *216*, 110536.
- [92] Y. Liu, P. Bhattarai, Z. Dai, X. Chen, *Chem. Soc. Rev.* **2019**, *48*, 2053.
- [93] L. Qin, S. Jiang, H. He, G. Ling, P. Zhang, *J. Controlled Release* **2020**, *318*, 50.